Rapid adsorption of cobalt (II) by 3-aminopropyltriethoxysilane modified halloysite nanotubes

Xin Wang, Yuantao Chen[†], Wei Zhang, Wenfang He, Jian Wang, and Biqing Chen

Department of Chemistry, Qinghai Normal University, Xining 810008, P. R. China

Abstract–The adsorption of cobalt (II) by 3-aminopropyltriethoxysilane (APTS) modified halloysite nanotubes (HNTs) was studied. The modified halloysite was characterized by Fourier transform infrared spectroscopy (FT-IR), X-Ray diffraction (XRD) and thermogravimetry (TG). In addition, a batch method was used to study the adsorption behavior and the mechanism of removal Co (II) by modified HNTs; the effective factors influencing the adsorption process including adsorbent concentration, contact time, initial pH, temperature and the initial concentration of Co (II) have been investigated. The results showed that the APTS was successfully grafted on the HNTs surface. The modified HNTs exhibited rapid adsorption speed, which reached the adsorption equilibrium within 30 min. The adsorption capacity of the adsorbent increased significantly with the increase of pH. The adsorption data of Co (II) on the modified HNTs are well consistent with the Langmuir model and the pseudo-second-order kinetic model.

Keywords: Halloysite Nanotube, 3-Aminopropyltriethoxysilane, Modification, Cobalt, Adsorption

INTRODUCTION

The development of nuclear energy has created a worldwide problem from the processing of radioactive nuclear waste. Radioisotope of cobalt is produced during the burn-up of nuclear fuel in a reactor, and is of great concern from the environmental point of view [1]. Traces of this radionuclide may remain in the waste solution and negatively affect humans and other living creatures. Exposure to Co (II) is extremely irritating to the skin both on contact and by provoking an allergic reaction which sensitizes the skin to further contact. It is also irritating to the eyes and mucous membrane, causing severe nasal discomfort, and often leading to perforation of the nasal septum. The threshold limit value for cobalt fume and dust exposures is 0.1 mg/ml in the U.S. [2]. The limited value for cobalt in wastewater discharge is 1 mg/L in China [3], and the threshold limit value for cobalt in irrigation water is 0.1 mg/L [4]. This radionuclide is not biodegradable, so there is a desperate need to find a way to remove it from waste water. Several conventional methods, such as chemical precipitation, ion exchange, membrane separation and adsorption, have been applied for heavy metal ion removal from effluents [5]. Among these, adsorption can be a suitable alternative approach to treating industrial waste water, especially if the adsorbent used is a low-cost material that does not need pre-treatment [6]. Many adsorbents have been studied in the removal of Co (II), including coal powder [1], activated carbon [7], silica gel [8] and so on.

Halloysite, a type of naturally occurring clay mineral with a nanotubular structure [9], possesses a two-layer structure formed by a corner sharing $[SiO_4]$ tetrahedral layer and an edge sharing $[AlO_6]$ octahedral layer. Each of these two layers is separated by a monolayer of interlayer water molecules [10]. The interlayer water is weakly held, so that halloysite-10Å can readily transform to halloysite-7 Å [11]. HNTs have a relatively high specific surface area, high porosity, and high cation-exchange capacity [12]. Their exceptional physical and chemical properties make them suitable in electronics, polymers, catalysis, adsorption, biology and medicine [13-17].

As the adsorbents, HNTs could absorb cationic dyes [18,19] and Cr (VI) [20]. As the support of the photocatalysts, HNTs could be attached with TiO_2 nanoparticles to decompose methylene blue dye, NO_x gas, toluene, methanol and acetic acid [21]. To date, halloysite has been modified by a variety of guest molecules such as phenylphosphonic acid [22], γ-methacryloxypropyl trimethoxysilane [23], methacrylic acid [24] and bis-(triethoxysilylpropyl)-tetrasulphide [25]. These studies have changed the performance of halloysite as the adsorbents.

In the present work, we prepared a novel adsorbent by grafting 3-aminopropyltriethoxysilane (APTS) onto HNTs and studied the ability of modified HNTs to remove Co (II) from aqueous solution. The factors affecting the Co (II) adsorption capacity were investigated in detail, and the adsorption mechanism was elucidated through the adsorption behavior.

MATERIALS AND METHODS

1. Samples

The halloysite nanotube (HNTs) samples were provided by Guangdong Province, China. 3-Aminopropyltriethoxysilane was purchased from Jiangsu Province, China. Cobalt iron solution was prepared by dissolving cobalt chloride hexahydrate ($CoCl_2 \cdot 6H_2O$) in distilled water. All other chemicals were analytical reagent grade without further treatment and all solutions were prepared using distilled water.

[†]To whom correspondence should be addressed.
E-mail: chenyt@qhnu.edu.cn

2. Modification of HNTs

HNTs were modified by the following method: 2 mL of APTS was added to 30 mL of methanol in a conical flask, and dispersed for 20 min by ultrasonic apparatus. About 2 g of HNTs powder was added to the above solution and the mixture was sonicated for 1 h at room temperature. Then, the suspension was stirred for 8 h at 120 °C. The modified HNTs were filtered and thoroughly washed twice with methanol, then dried for 24 h at 120 °C.

3. Characterization Techniques

FT-IR spectra were recorded on a Nicolet iS50 in the 400-4,000 cm^{-1} range in transmittance mode. KBr pellets were prepared by crushing the solids around spectroscopic grade KBr .

X-ray diffraction (XRD) patterns were obtained by using a LabX XRD-6000 diffractometer with a Cu Kα radiation (λ=0.154 nm). The powdered samples were placed on aluminum sample-holders. The measurements were performed in the continuous scan mode at 20 kV and 20 mA.

Thermogravimetric analysis was performed in nitrogen using a Netzsch Sta 449f3 thermal analyzer at a heating rate of 10 °C/min.

4. Adsorption Experiments

We explored the effects of the concentration of HNTs-APTS, the pH of the medium, the temperature, the contact time on the adsorption and the initial concentration of Co (II). The experiments involved using static adsorption method in polyethylene centrifuge tubes under ambient conditions. All experiments were carried out by a certain of 60 mg/L of Co (II) and 6 g/L of HNTs-APTS. The pH of each sample was adjusted to desired values by adding a tiny amount of 0.01 or 0.1 mol/L HCl or NaOH. The suspensions were agitated for 24 h on a thermostatted shaker of 180 rpm at constant temperature. And then centrifuged at 8,000 r/min for 30 min to separate the solid from liquid phases totally. The concentration of Co (II) was analyzed by UV-VIS spectrophotometer.

The amount of Co (II) adsorbed at equilibrium (q$_e$, mg/g) or at time (q$_t$, mg/g), distribution coefficient K$_d$ and removal efficiency (Y, %) was calculated by using the following equations, respectively:

$$k_d = \frac{C_0 - C_e}{C_0} \times \frac{V}{m} \tag{1}$$

$$q_e = \frac{(C_0 - C_e) \times V}{m} \tag{2}$$

$$q_t = \frac{(C_0 - C_t) \times V}{m} \tag{3}$$

$$Y\% = \frac{C_0 - C_e}{C_e} \times 100\% \tag{4}$$

where C$_0$, C$_t$, and C$_e$ (mg/L) are the initial, time t, and equilibrium concentrations of Co (II) solution respectively; K$_d$ is the distribution coefficient; V (L) is the volume of Co (II) solution and m (g) is the weight of adsorbent. The distribution coefficient, K$_d$ values, is a function of the solid amount and sorption percentage.

RESULTS AND DISCUSSION

1. Characterizations

1-1. FT-IR

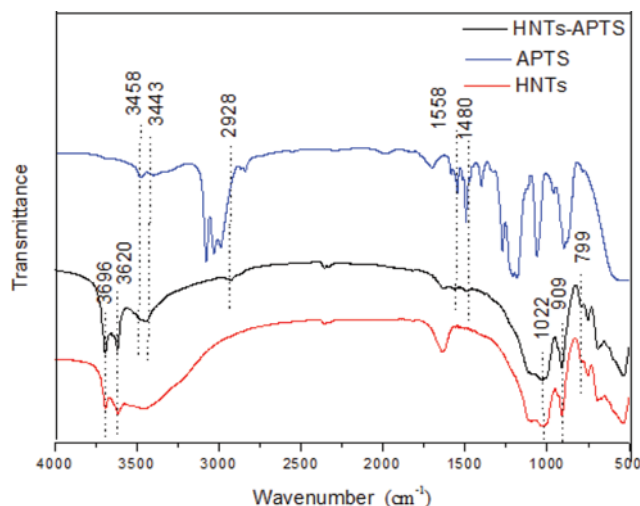Fig. 1 shows the FT-IR spectra of pure APTS, HNTs before and

Fig. 1. FTIR spectra of the APTS, HNTs and HNTs-APTS.

after modification with APTS. From Fig. 1, characteristic FT-IR adsorption peaks of HNTs were resolved in all materals. These peaks include the symmetrical stretching of Si-O-Si at 799 cm^{-1}, the in-plane Si-O stretching at 1,022 cm^{-1}, the perpendicular Si-O stretching at 1,114 cm^{-1}, the O-H stretching of inner surface hydroxyl groups at 3,620 cm^{-1}, the O-H stretching of inner hydroxyl groups at 3,696 cm^{-1} and the O-H deformation of inner hydroxyl groups at 909 cm^{-1}. Compared to the unmodified HNTs, HNTs-APTs have new peaks, including the symmetrical stretching of C-H in methylene at 2,928 cm^{-1}, the deformation of C-H$_2$ at 1,480 cm^{-1}, the bending vibration of N-H in primary amine at 1,558 cm^{-1}, and there is a double peak phenomenon at 3,300-3,500 cm^{-1}, indicating primary amine in HNTs-APTS. These peaks were correlated to the chemical bonds of APTS and clearly illustrated that the APTS was successfully loaded on the HNTs.

1-2. XRD

Fig. 2 displays the XRD patterns of HNTs and HNTs-APTS. From Fig. 2, both of them exhibit the characteristic plane of HNTs with the plane at 2θ=12.52°, corresponding to the planes (001), with

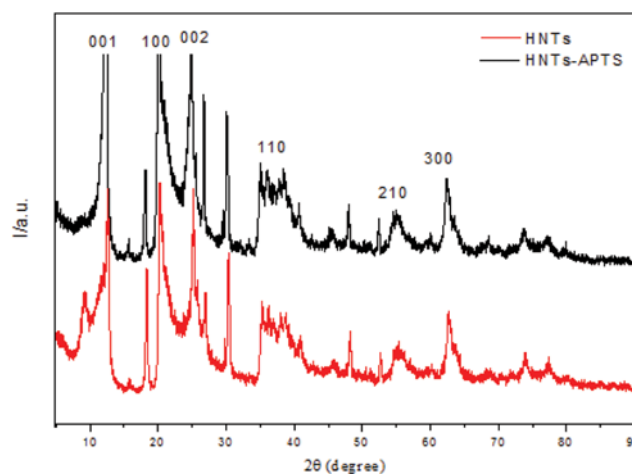Fig. 2. XRD patterns of HNTs and HNTs-APTS.

d=0.7 nm. This HNT basal reflection results from its tubular morphology and small crystal size (L) of 21.71 nm that was calculated from the Scherrer relation [26]. In addition, the XRD pattern of HNTs also shows other planes at $2\theta=20.29^{\circ}$ and 25.1°, corresponding to the (100) and (002) planes with d values of 0.44 and 0.35 nm. Furthermore, there are also other planes at $2\theta=35.20^{\circ}$, 54.73° and 62.76°, corresponding to the planes (110), (210) and (310) with d=0.255, 0.168, 0.148 nm, respectively. Based on the database, it has been found that HNTs used in this study are referred to as halloysite-7 Å with a dehydrated formation [27]. But there is a plane at about $2\theta=9.11^{\circ}$ for hydrated particles, which illustrates the HNTs used for this study are not dehydrated completely. For HNTs-APTS, characteristic planes are found at $2\theta=12.29^{\circ}$, 20.14° and 24.89° with d values of 0.72, 0.44 and 0.36 nm. These planes are corresponding to the planes (001), (100), and (002), respectively. Also at $2\theta=35.08^{\circ}$, 54.83° and 62.40°, corresponding to the planes (110), (210) and (310) with d=0.256, 0.167, 0.149 nm, respectively. As we can see, the (001) plane of HNTs-APTS slightly had lower angles at $2\theta=12.515^{\circ}$ relative to that of HNTs at $2\theta=12.29^{\circ}$. This phenomenon reveals that HNTs-APTS shows slightly better dispersion than HNTs [28]. So the adsorption capacity of HNTs-APTS becomes good. This is because the agglomeration tendency of HNTs-APTs decreases, which might assist its dispersion in the solution. In addition, the XRD pattern of HNTs-APTS remains unchanged compared to that of HNTs, indicating that APTS was not intercalated into the interlayer spaces [29]. This result is in accordance with the observation that APTS was only grafted onto the surface hydroxyl groups of the internal surfaces edges and external surfaces of tubular halloysite under mild reaction conditions [30].

1-3. TG

The thermal analysis measurements of HNTs and HNTs-APTS are shown in Fig. 3. According to the TG curves of HNTs, there is a large amount of weight loss (about 3.0%) from 30 °C to 80 °C, which is typical of the free water of halloysite. From 100 °C to 500 °C, which can be attributed to the loss of bound water, with a mass loss of 10%. In contrast to HNTs, thermal analysis of HNTs-APTS revealed a two-step curve, with a gradual weight loss at the low-temperature region followed by a steep mass loss at the higher tem-
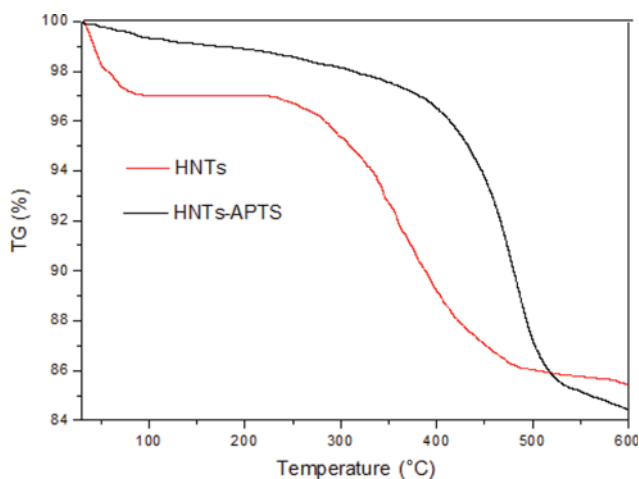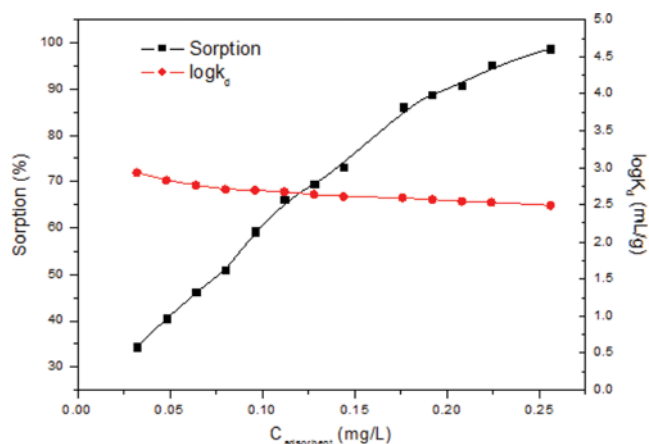

Fig. 4. Adsorption of Co (II) on HNTs-APTS as a function of solid content.

peratures. The mass loss (of about 2%) observed between 30 °C and 200 °C was assigned to bound water of HNTs and silane coupling agent desorption of coordinate water molecules [31]. The mass loss (of about 13%) from 200 °C to 500 °C was associated with the decomposition of the APTS grafted onto SiOH and AlOH groups on edges or external surface, the oligomerized APTS, and the APTS grafted on AlOH groups at the internal surface of the lumen [32].

2. Effect of Adsorbent Concentration

Adsorbent concentration is an important factor for adsorption capacity. The effect of the adsorbent concentration was investigated by addition of various amounts of HNTs-APTS in Co (II) aqueous solution at room temperature. As shown in Fig. 4, along with the increasing of the concentration of HNTs-APTS, the adsorption efficiency of Co (II) increased gradually. With the increasing of concentration, the adsorption sites of Co (II) on the adsorbent also increase, the adsorption quantity increases. From Fig. 4, we can also see that the distribution coefficient K_d decreased gradually with the concentration increased. This might be because with the changing of the concentration, the functional groups at the surface of HNTs-APTS will form compete or reunion. That is, when adsorption sites are increasing, they can raise adsorption rate for the removal of Co (II), but because of the compete or reunion of the increased functional groups, it can also make adsorption capacity decreased of HNTs-APTS for the removal of Co (II).

3. Effect of Contact Time and Adsorption Kinetic

The adsorption of Co (II) on HNTs-APTS as a function of contact time is shown in Fig. 5(a). Obviously, the results show that the adsorption is rapid for the first 10 min and finally attains equilibrium for about 30 min. And the adsorption capacities reached 11.1 mg/g for 5 min and reached 12.3 mg/g for 10 min. This experiment result shows that the adsorption of Co (II) on modified halloysite is mainly physical adsorption, not chemical adsorption. The results indicate the adsorbent has a rather rapid adsorption rate and a contact time of 1 h is sufficient for the adsorption of Co (II). The pseudo-first-order kinetic model and the pseudo-second-order kinetic model were used to fit the adsorption kinetic data. The models can be described as the following equations:

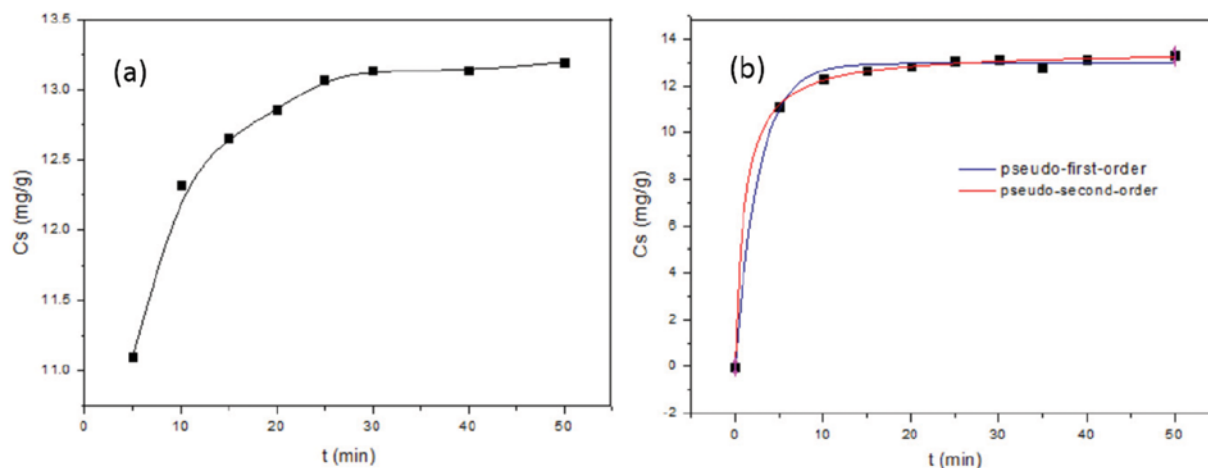Fig. 3. Thermal analysis measurements of HNTs and HNTs-APTS.

Fig. 5. Adsorption of Co (II) on HNTs-APTS as a function of contact time (a) pseudo-first-order and pseudo-second-order models (b).

$$\ln(q_e - q_t) = \ln q_e - k_1 t \tag{5}$$

$$q_t = \frac{k_2 q_e^2 t}{1 + k_2 q_e t} \tag{6}$$

where k_1 and k_2 are the pseudo-first-order and pseudo-second-order rate constants for adsorption, q_t and q_e (mg/g) are the amount of solute at time t (min) and at equilibrium, respectively.

The adsorption kinetic of removal Co (II) by HNTs-APTS is shown in Fig. 5(b). The results show that the correlation coefficient R^2 (0.9988) for the pseudo-second-order model is higher than that of the pseudo-first-order (0.9969), indicating that the present adsorption system can be defined by the pseudo-second-order kinetic model in the adsorption step.

The equilibrium time of Co (II) adsorption on the HNTs-APTS compared with other adsorbents is given in Table 1. Note that the equilibrium time of Co (II) adsorption on the HNTs-APTS is much shorter than that of other adsorbents.

4. Effect of Initial pH

The removal of Co (II) as a function of pH was examined over an initial pH range of 1-12, and the results are shown in Fig. 6. The adsorption capacity did not significantly change between pH 1.43 and 3.54, and then it increased quickly as the initial pH increased from 3.64 to 7.02. Afterward, between pH 7.02 and 11.4,

the adsorption capacity did not significantly change again. This performance may be associated with the surface functional groups and surface charge of HNTs-APTS. Amino groups are of alkalescence and can be protonated, thus allowing adsorption to occur through electrostatic attraction at higher pHs [10]. Co (II) can exist in a series of different steady forms such as $Co(OH)^+$, $Co(OH)_2$, $Co(OH)_3^-$, and the existing form mainly depended upon the solution pH. Generally speaking, Co (II) was major specie at pH below 2. $Co(OH)_2$ and $Co(OH)_3^-$ came into being when pH was higher than 8.8. As the pH further increased, Co (II) hydrolyzed to $Co(OH)_3^-$. Co (II) removal rates maintained a high value when pH was higher than 7, which was attributed mainly to electrostatic attraction between the negatively charged $Co(OH)_3^-$ and the positively charged amino functional groups caused by strong protonation on the adsorbent surface. However, when the pH was higher than 10, the main existing form of Co (II) was $Co(OH)_2$; because of the impact of precipitation, the concentration of Co (II) also decreased. When the pH was reduced to less than 2, electrostatic interaction was reduced as Co (II) mainly existed in the form of $CoCl_2$. At pH higher than 7, deprotonation processes occurred on the adsorbent, resulting in

Table 1. The equilibrium time of Co (II) adsorption on the HNTs-APTS compared with other adsorbents

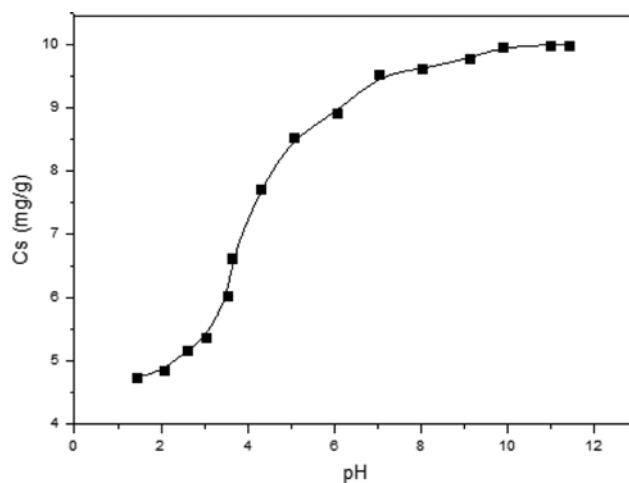| Adsorbent	Equilibrium time	Reference
Pakistani coal powder	2 h	[1]
Magnetic halloysite	5 h	[33]
Magnetic illite	8 h	[34]
HNTs	4 h	[35]
Montmorillonite	1 h	[36]
Modified zeolite	6 h	[37]
Surface-grafted Co (II)-imprinted polymer	5 h	[38]
HNTs-APTS	0.5 h	This study

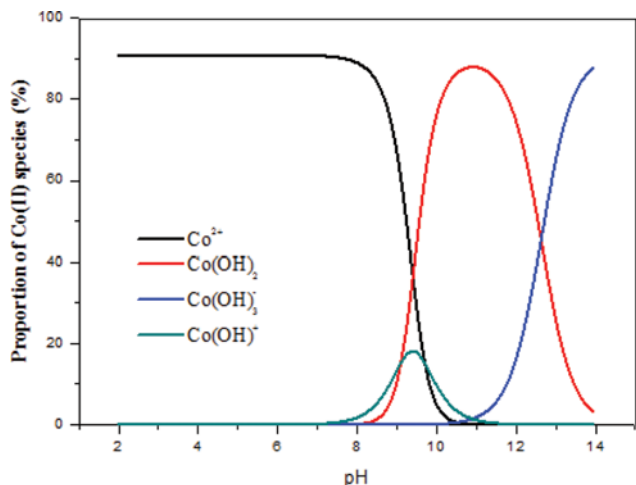Fig. 6. Adsorption of Co (II) on HNTs-APTS at different pH.

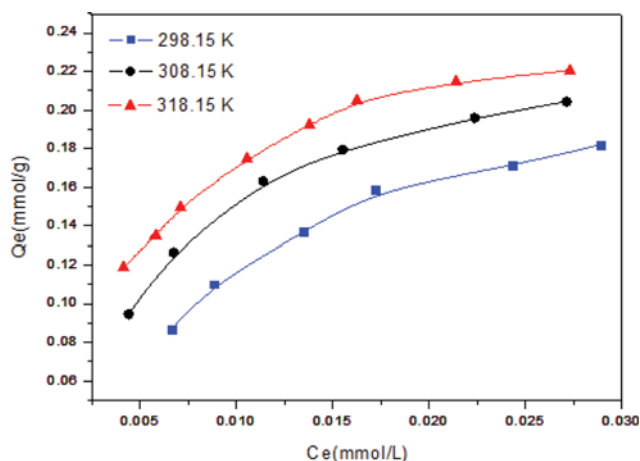Fig. 7. Distribution of Co (II) species at different pH.

Fig. 8. Adsorption of Co (II) on HNTs-APTS as a function of temperature and the initial concentration of Co (II).

the increase of Co (II) uptake. From Fig. 7, we can see different forms of Co (II) at different pH. All in all, the optimum pH for removal of Co (II) was found to be 7 to 9. The modified adsor-

bent had a relatively broader pH range.

5. Effect of Temperature and the Initial Concentration of Co (II)

Fig. 8 shows the adsorption capacity of Co (II) onto HNTs-APTS at 298.15 K, 308.15 K, and 323.15 K, respectively. Obviously, we can reach the conclusion that the concentration of Co (II) influenced the adsorption capacity no matter at which temperature. With the concentration increasing, the adsorption capacity also increased. This conclusion was to be expected. Because for a certain amount of adsorbent having limited total available adsorption sites, the concentration increased, resulting in the increase of adsorption capacity of Co (II) until equilibrium was reached.

From Fig. 8, with the temperature increasing from 298.15 K to 318.15 K, the adsorption capacity also increased. This fully demonstrated that the adsorption of Co (II) on HNTs-APTS was endothermic.

6. Adsorption Thermodynamics

For the adsorption experiment, adsorption isotherms are essential. To study the adsorption thermodynamics, both Langmuir model and Freundlich model were applied to fit the experimental data.

The equations were as follows:

$$\frac{C_e}{C_s} = \frac{1}{bC_{s\,max}} + \frac{C_e}{C_{s\,max}} \tag{7}$$

$$\log C_s = \lg K_F + n \lg C_s \tag{8}$$

where C_e (mg/L) is the equilibrium concentration of Co (II). C_s (mg/g) is the equilibrium adsorption capacity, $C_{s\,max}$ (mmol/g) is the maximum amount of Co (II) per weight unit. b (L/mol) is the Langmuir adsorption equilibrium constant. K_F ($mol^{1-n}/L^n/g$) is the adsorption capacity when Co (II) equilibrium concentration equals to 1 and n represents the degree of dependence of adsorption with equilibrium concentration.

The fitting plots of Langmuir and Freundlich isotherm models for Co (II) adsorption on modified HNTs are shown in Fig. 9. The calculated isotherm parameters along with correlation coefficients are given in Table 2. It is observed that the maximum adsorption capacity of the adsorbent calculated from the Langmuir model can reach 0.3 mmol/g. The correlation coefficient R^2 of Langmuir isotherm model is higher than that of Freundlich isotherm model,
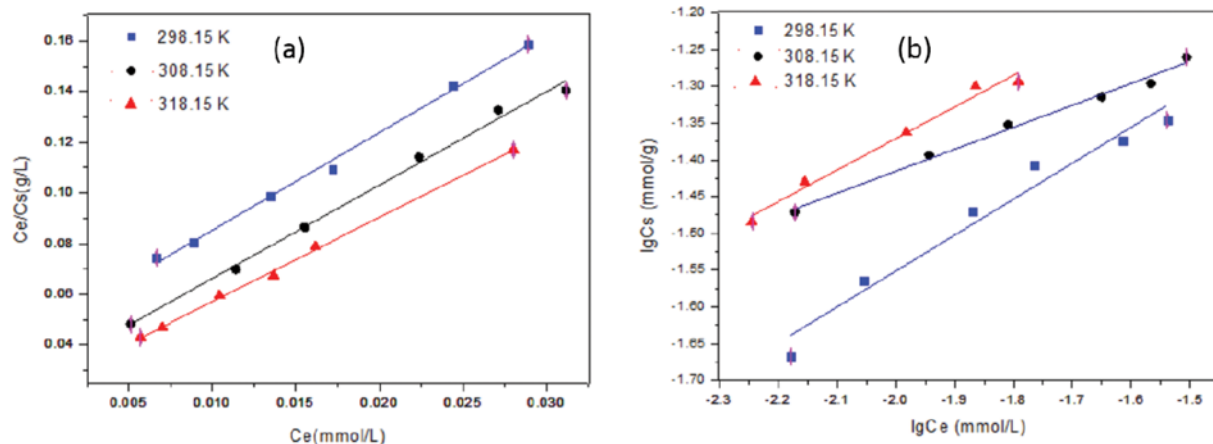

Fig. 9. Langmuir (a), Freundlich (b) isotherms of Co (II) adsorption.

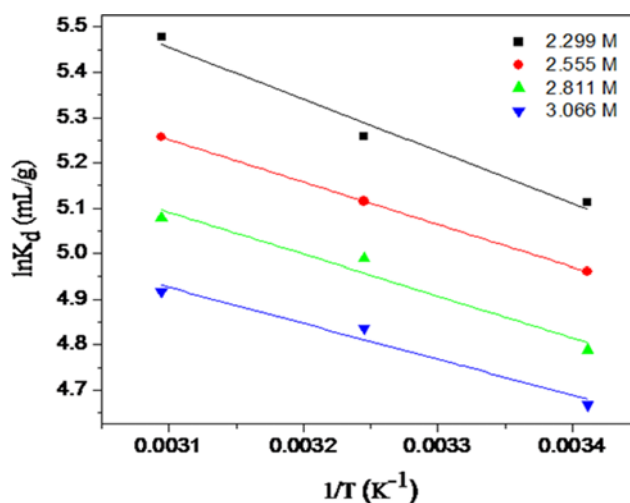**Table 2. Langmuir and Freundlich parameters for Co (II) adsorption**

T (K)	Langmuir			Freundlich		
	$C_{s\,max}$ (mmol/g)	b (L/mmol)	R^2	K_F (mmol^{1-n}/L^n/g)	n	R^2
293.15	0.259	79.36	0.995	0.269	0.49	0.954
303.15	0.271	125.94	0.993	0.154	0.3	0.987
313.15	0.3	140	0.998	0.31	0.43	0.978

Table 3. The Co (II) adsorption capacity of the HNTs-APTS compared with other adsorbents

Adsorbent	Sorption capacity (mg/g)	Reference
Natural zeolites	14.38	[40]
Crab shell	20.47	[41]
Magnetic halloysite	13.78	[33]
Synthetic HAP	20.19	[42]
HNTs-APTS	17.67	This study
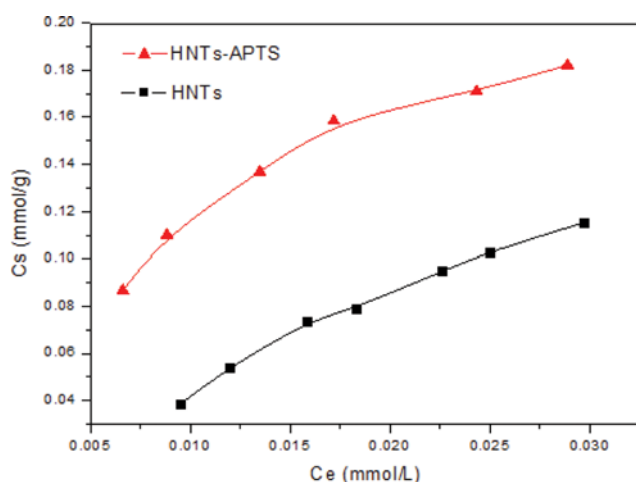
Fig. 10. The Co (II) adsorption capacity of the HNTs-APTS compared with HNTs.

Fig. 11. Linear plots of lnKd vs. Ce of Co(II) adsorption onto HNTs-APTs.

indicating that the adsorption was monolayer adsorption process. In addition, the Langmuir constant b has positive value, implying a favorable adsorption system, and the Freundlich constant n is lower than 1, implying a nonlinear adsorption process occurs on adsorbent [39]. Under the temperature of 293.15 K, 303.15 K and 313.15 K, it is clear that the adsorption capacity of modified HNTs becomes higher with the temperature increasing. This illustrates that elevated temperature is conducive to the adsorption process. Table 3 shows the Co (II) adsorption capacity of some kinds of adsorbents. Note that the Co (II) adsorption capacity of HNTs-APTS

is not the highest one than those of other adsorbents, but it is obviously shown in Fig. 10, compared to HNTs, that the adsorption capacity has gotten high.

The thermodynamic parameters (ΔH^θ, ΔG^θ, ΔS^θ) for Co (II) sorption on HNTs-APTS can be obtained from the following equations:

$$\lg k_d = \frac{\Delta S^\theta}{R} - \frac{\Delta H^\theta}{RT} \tag{9}$$

$$\Delta G^\theta = \Delta H^\theta - T\Delta S^\theta \tag{10}$$

where ΔG^θ (kJ/mol) is Gibbs free energy; R (8.314 J/mol/K) is perfect gas constant; T (K) is absolute temperature; K_d is the distribution coefficient; ΔH^θ (kJ/mol) is enthalpy change; ΔS^θ (J/mol /k) is entropy change.

The values of ΔH^θ and ΔS^θ are calculated from the slope and intercept of $\ln K_d$ against 1/T. From Table 4, the positive value of ΔH^θ indicates that the adsorption process is endothermic. The value of ΔS^θ is positive, which confirms the increased randomness at the solid-solution interface during Co (II) adsorption. Table 4

Table 4. The thermodynamic data of Co (II) adsorption on HNTs-APTS at different initial concentrations

C_0 (mmol/L)	ΔS^θ (J/mol/K)	ΔH^θ (KJ/mol)	ΔG^θ (KJ/mol)		
			298.15 K	308.15 K	318.15 K
1.36×10^{-5}	89.20	11.39	−15.2	−16.09	−16.99
2.44×10^{-5}	83.72	9.82	−15.14	−15.98	−16.82
2.99×10^{-5}	82.06	9.49	−14.98	−15.83	−16.65

also shows that ΔG^{θ} is negative, indicating that the adsorption is feasible and spontaneous.

CONCLUSIONS

Halloysite nanotubes were modified by 3-aminopropyltriethoxysilane to form a new adsorbent. The removal of Co (II) from aqueous solutions by HNTs-APTS was studied as a function of adsorbent concentration, contact time, pH, temperature and the initial concentration of Co (II). The experimental results show that (1) The removal of Co (II) from solution is favorable at high pH, and the best range for pH is 7 to 9. (2) The adsorption of Co (II) is rather fast, illustrating the process is physical absorption, and the kinetic data is well fitted by pseudo-second-order kinetic model. (3) In the whole range of Co (II) concentration, the Langmuir isotherm equation was obeyed well with high value of correlation coefficient. (4) High temperature favors the adsorption of Co (II) onto HNTs-APTS, indicating the adsorption process is endothermic. (5) The value of Gibbs free energy is negative, showing that this process is spontaneous.

REFERENCES

1. R. Qadeer, *J. Radioanal Nucl. Chem.*, **295**, 2021 (2013).
2. Y. V. Hete, S. B. Gholse and R. U. Khope, *J. Mater. Sci. Eng. Part B*, **1**, 117 (2011).
3. H. Du, *Central South University*, Chang Sha, Hu Nan provice in China (2013).
4. V. D. Karate and K. V. Matathe, *J. Hazard. Mater.*, **157**, 209 (2008).
5. M. A. Tofighy and T. Mohammadi, *Korean J. Chem. Eng.*, **32**, 292 (2015).
6. S. H. Khorzughy, T. Eslamkish, F. D. Ardejani and M. R. Heydartaemeh, *Korean J. Chem. Eng.*, **32**, 88 (2015).
7. S. Oh and D. S. Kim, *Environ. Sci. Health Part B*, **49**, 710 (2014).
8. Y. T. Fang, T. Liu, Z. C. Zhang and X. N. Gao, *Renew. Energy*, **63**, 755 (2014).
9. P. Luo, J. Sh. Zhang, B. Zhang, J. H. Wang, Y. F. Zhao and J. D. Liu, *Ind. Eng. Chem. Res.*, **50**, 10246 (2011).
10. Y. Y. Du and P. W. Zheng, *Korean J. Chem. Eng.*, **31**, 2051 (2014).
11. P. Luo, B. Zhang, Y. F. Zhao, J. H. Wang, H. Q. Zhang and J. D. Liu, *Korean J. Chem. Eng.*, **28**, 800 (2011).
12. P. W. Hu and H. M. Yang, *Phys. Chem. Miner.*, **39**, 339 (2012).
13. M. L. Du, B. C. Guo and D. M. Jia, *Polym. Int.*, **59**, 574 (2010).
14. A. D. Hughes and M. R. King, *Langmuir*, **26**, 12155 (2010).
15. Y. M. Lvov, D. G. Shchukin and R. R. Price, *ACS Nano*, **2**, 814 (2008).
16. L. Wang, J. Chen, L. Ge, Z. Zhu and V. Rudolph, *Energy Fuels*, **25**, 3408 (2011).
17. R. Zhai, B. Zhang, L. Liu, Y. D. Xie, H. Q. Zhang and J. D. Liu, *Catal. Commun.*, **12**, 259 (2010).
18. M. F. Zhao and P. Liu, *Micropor. Mesopor. Mater.*, **112**, 419 (2008).
19. P. Luo, Y. F. Zhao, B. Zhang, J. D. Liu, Y. Yang and J. F. Liu, *Water Res.*, **44**, 1489 (2010).
20. J. H. Wang, X. Zhang, B. Zhang, Y. F. Zhao, R. Zhai, J. D. Liu and R. F. Chen, *Desalination*, **259**, 22 (2010).
21. Y. Y. Du and P. W. Zheng, *Korean J. Chem. Eng.*, **31**, 2051 (2014).
22. Y. H. Tang, Sh. Q. Deng, L. Ye, Ch. Yang, Q. Yu, J. N. Zhang and Ch. B. Zhao, *Compos. Part A-Appl. S.*, **42**, 345 (2011).
23. P. Pasbakhsh, H. Ismail, M. A. Fauzi and A. A. Bakar, *Appl. Clay. Sci.*, **48**, 405 (2010).
24. B. Ch. Guo, Y. D. Lei, F. Chen, X. L. Liu, M. L. Du and D. M. Jia, *Appl. Surf. Sci.*, **255**, 2715 (2008).
25. S. Rooj, A. Das, Va. Thakur, R. N. Mahaling, A. K. Bhowmick and G. Heinrich, *Mater. Des.*, **31**, 2151 (2010).
26. P. Pasbakhsh, H. Ismail, M. N. Ahmad Fauzi and A. Abu Bakar, *Appl. Clay Sci.*, **48**, 3 (2010).
27. Y. Dong, D. Chaudhary, H. Haroosh and T. Bickford, *J. Mater. Sci.*, **46**, 6148 (2011).
28. H. J. Haroosh, D. Yu, D. S. Chaudhary, G. Ingram and S. Yusa, *Appl. Phys. A*, **110**, 439 (2013).
29. H. L. Lun, J. Ouyang and H. Yang, *Appl. Clay. Sci.*, **4**, 44198 (2014).
30. B. Ch. Guo, Y. D. Lei, F. Chen, X. L. Liu, M. L. Du and D. M. Jia, *Appl. Surf. Sci.*, **255**, 5 (2008).
31. D. L. Wang, J. Yang, M. J. Tan, Y. H. Li and W. L. Li, *Package. J.*, **2**, 19 (2010).
32. P. Yuan, P. D. Southon, Z. W. Liu, M. E. R. Green, J. M. Hook, S. J. Antill and C. J. Kepert, *J. Phys. Chem. C.*, **112**, 15748 (2008).
33. Ch. L. Hu, Y. T. Chen, W. Zhang, P. P. Wang and J. Wang, *Acta Sci. Circumst.*, **35**, 2814 (2014).
34. Ch. L. Hu, Y. T. Chen, W. Zhang, J. Xiao, Y. L. Chi and W. F. He, *Chem. Ind. Eng. Prog.*, **33**, 2412 (2014).
35. Z. M. Li, T. F. Chen and F. Ch. Yi, *J. Southwest Univ.*, **22**, 35 (2007).
36. Z. J. Zhang, Y. Deng, Z. Y. Zhao and G. Ch. Lv, *Environ. Sci. Technol.*, **36**, 168 (2013).
37. J. X. Che, L. P. Kuai and X. P. Wang, *Ind. Water Treat.*, **31**, 70 (2011).
38. Y. Liu, J. Gao, Ch. X. Li, J. M. Pan, Y. Sh. Yan and J. M. Xie, *Chin. J. Chem.*, **28**, 552 (2010).
39. C. L. Chen, X. L. Li, D. L. Zhao, X. L. Tan and X. K. Wang, *Colloids Surf., A*, **302**, 450 (2007).
40. E. Erdem, N. Karapinar and R. Donat, *J. Colloid Interface Sci.*, **280**, 312 (2004).
41. K. Vijayaraghavan, M. Thilakavathi, K. Palanivelu and M. Velan, *Environ. Technol.*, **26**, 274 (2005).
42. I. Smiciklas, S. Dimovic, I. Plecas and M. Mitric, *Water Res.*, **40**, 2272 (2006).